PREDICTIVE CONTROLLER FOR OPTIMAL RENEWABLE HYDROGEN INJECTION INTO THE NATURAL GAS NETWORK

Carlo Carcasci[1], Michele Francesconi[1], Agostino Gambarotta[2,3], Gabriele Guzzo[1], Emanuela Marzi[2]*, Mirko Morini[2], Costanza Saletti[2]

[1]University of Florence, Department of Industrial Engineering (DIEF), Florence, Italy.

[2]University of Parma, Department of Engineering for Industrial Systems and Technologies (DISTI), Parma, Italy.

[3]University of Parma, Center for Energy and Environment (CIDEA), Parma, Italy.

*Corresponding Author: emanuela.marzi@unipr.it

ABSTRACT

The energy transition is fostering the penetration of renewable energy sources into existing energy networks. In this context, Power-to-Gas solutions, which can convert renewable electricity into green hydrogen, are becoming prominent, emphasizing the significance of gas and electricity network interoperability. During the transitional phase, the gas network can provide flexibility to the energy system by absorbing hydrogen, thus preventing the curtailment of electricity. However, leveraging existing infrastructures cannot disregard compliance with gas quality standards represented by the Wobbe Index, the specific gravity and the Higher Heating Value of the gas. Given the non-negotiable nature of constraints regarding user safety and the inherent unpredictability of renewable energy availability and user demand, successful integration of energy networks necessitates the deployment of intelligent control strategies. This paper presents a novel control strategy based on Model Predictive Control, for the optimal management of hydrogen generation through an electrolyzer, and its subsequent injection into the existing gas network. The test case represents an integrated energy system that comprises renewable energy generation, the electrical grid, an electrolyzer, and the gas network. It was designed to mirror real-world conditions by including unexpected disturbances in renewable energy generation and user demand. The feasibility of the proposed controller is verified through a Model-in-the-Loop simulation platform. The results underscore its efficacy in maximizing the usage of renewable energy while ensuring gas quality standards, also considering the dynamic operation of the gas network. The results affirm its practical viability in real-world energy transition scenarios, paving the way for further exploration into more complex systems in future research.

1 INTRODUCTION

To address the necessity to reduce carbon dioxide emissions in the energy sector, significant efforts are being made to foster the penetration of decentralized and non-programmable renewable energy sources (RES). These changes are reshaping the structure of existing energy systems, which necessitate enhanced flexibility to manage the mismatch between energy generation and consumption. In this framework, Power-to-Gas technologies enable the integration of different sectors, such as electricity, heating, and transportation, by converting surplus electricity into gaseous energy vectors, e.g. green hydrogen or methane. Although global interest in green hydrogen is growing, before it can replace traditional fuels, well-developed infrastructures for its transport and utilization need to be established (Neumann *et al.*, 2023). In the transitional phase, blending hydrogen into existing infrastructures can encourage the development of a market while offering flexibility to the electricity grid (Cristello *et al.*, 2023). Erdener *et al.* (2023) showed the advantages and limitations of blending hydrogen into the existing natural gas network and highlighted the current regulatory limitations of doing so.

The different properties of natural gas and hydrogen encouraged researchers to develop mathematical models capable of tracking gas composition to investigate the quality and fluid-dynamic implications of transporting a blend. For instance, Chaczykowski *et al.* (2018) compared the implicit solution of the

https://doi.org/10.52202/077185-0007

advection equation to the *batch tracking* method showing the effectiveness of both methods. The former presents numerical instability if there is a sharp variation in boundary conditions, while the latter avoids numerical instability, but as a drawback the error cumulates as the batch moves forward. Zhang *et al.* (2022) proposed and validated a method for determining the maximum discretization length to mitigate numerical instability caused by the advection equation when implementing localized hydrogen injection. A similar model was presented by Mhanna *et al*. (2022): the authors integrated the model into a sequential linear programming algorithm to coordinate the operation of electrical and gas networks in case of multiple hydrogen injections, showing improved performance compared to standard algorithms. Other studies proposed an energy approach method applied to various gas network scenarios. For instance, Guandalini *et al.* (2017) studied a high-pressure pipeline system, Cheli *et al*. (2021) analyzed a fictitious low-pressure distribution network, and Guzzo *et al.* (2022) examined a real gas distribution network encompassing medium- and low-pressure levels. The studies revealed that low hydrogen blends exhibit significant effects on velocities while having a minimal or negligible impact on pressure losses. Besides, when related to its energy content, the compression of a natural gas and hydrogen blend needs a larger amount of power (Morini *et al.*, 2009) and its flow in pipes dissipates a larger amount of energy (Cadorin *et al.*, 2010). In addition, substantial impacts are noted on the Higher Heating Value (HHV) and the Wobbe Index, underscoring the importance of maintaining these values within regulatory limits. Cheli *et al*. (2021) emphasized the necessity for control strategies to address these issues, although no specific solutions have been proposed. In this context, Zhou *et al*. (2022) developed and compared different control laws for the operation of an integrated system with hydrogen generation from renewable energy and its blending into the natural gas network. They included outlet pressure and hydrogen concentration as controlled variables, which both need to meet certain requirements at the same time. Within the HyDeploy project (Isaac *et al.*, 2019), instead, a mixing loop is used to blend hydrogen with natural gas and obtain the desired hydrogen concentration in the blended gas before injecting it into natural gas pipelines. Nonetheless, in the context of integrated energy systems that include hydrogen generation, multiple energy carriers, and diverse technologies, the focus needs to be placed beyond hydrogen blending alone. Smart controllers emerge as key tools to enable the optimal management of such integrated energy systems. By using advanced algorithms and real-time data to make informed decisions, smart controllers can optimally coordinate the different system components, ensuring the achievement of determined objectives.

Among the existing control strategies, Model Predictive Control (MPC) is a model-based control strategy that enables optimal control following a certain objective, e.g. cost or energy minimization, by making use of an optimization algorithm with an integrated model of the system to control. This strategy has proven to be effective across various applications. However, to the best of the authors' knowledge, none of the existing studies on hydrogen blended in the natural gas network applies the MPC strategy to optimally control the generation of green hydrogen through an electrolyzer and its direct injection into the natural gas network. This work aims to fill this gap by developing an innovative control strategy based on MPC, capable of optimally managing a system that comprises renewable energy generation, hydrogen production, and its injection into the natural gas network, with a given maximum concentration. The controller is able to manage the system in real-time and adjust its operation according to its actual behavior. The controller is validated in a Model-in-the-Loop (MiL) configuration, using a detailed model of the system for emulating the behavior of a real system.

2 METHOD

This section presents the methods employed in this work. First, the mathematical models used for developing the simulation platform are described, then the MPC strategy is introduced, and lastly the optimization algorithms used for designing the controller are presented.

2.1 Simulation platform

The problem analyzed in this work deals with the smart control of an integrated system, aiming at the optimal management of hydrogen generation and injection into the existing gas network. An MiL setup was utilized to apply the controller to a model emulating the behavior of a real system. The model is presented in the following paragraphs: first, the gas network model is described, second, a brief overview of the energy system component models is introduced.

https://doi.org/10.52202/077185-0007

2.1.1 Gas network model

In the broader context of the study, a transient gas network model with localized hydrogen injection was developed. A set of partial differential equations is formed by the governing equations of the natural gas and hydrogen (NG-H_2) mixture flow through an isothermal pipeline, under the hypothesis of 1-D and unidirectional flow. These include the continuity equation (Eq. (1)) and momentum equation (Eq. (2)) for the gas mixture, along with the advection equation for H_2 mass concentration (Eq. (3)). It must be highlighted that the energy equation was neglected, as a constant temperature in the pipeline was assumed. These equations describe how pressure p, density ρ, and mass flow rate $\dot{m}$ change over time and space within a pipeline, which is characterized by diameter D and cross-sectional area A, and they can be written as follows

$$\frac{\partial \rho}{\partial t} + \frac{1}{A}\frac{\partial \dot{m}}{\partial x} = 0\,, \tag{1}$$

$$\frac{\partial p}{\partial x} + \frac{1}{A}\frac{\partial \dot{m}}{\partial t} + \frac{1}{A^2}\frac{\partial (\dot{m}^2/\rho)}{\partial x} + \frac{8f\dot{m}^2}{\rho \pi^2 D^5} = -p\frac{g \sin\theta}{ZR_\mathrm{g}T}\,, \tag{2}$$

$$\frac{\partial c_\mathrm{m}}{\partial t} + \frac{\dot{m}}{\rho A}\frac{\partial c_\mathrm{m}}{\partial x} = 0\,. \tag{3}$$

Under commonly used conditions in gas network modeling, Eq. (2) can be simplified by removing the term related to gravitational effects, under the assumption of a horizontally oriented pipeline, and removing the convective term, under the creeping motion hypothesis. In addition, Darcy friction factor f was approximated, under the hypothesis of fully turbulent flow, using the Nikuradse, Prandtl, von Karman (NPK) explicit formulation (Menon, 2005) expressed as follows

$$\frac{1}{\sqrt{f}} = -2\log_{10}\left(\frac{\varepsilon}{3.7D}\right). \tag{4}$$

To account for gas compressibility, the equation of state is used, which establishes the relationship between gas pressure p, density ρ and temperature T. From the real gas law, it can be written as

$$p = Z\rho R_\mathrm{g}T, \tag{5}$$

where R_g represents the gas constant of the NG-H_2 mixture. To describe Z (dimensionless compressibility factor), which accounts for the deviation of the real gas from ideal gas behavior, a Soave-modified Redlich-Kwong equation was employed (Soave, 1972).

The governing equations are numerically solved using a fully implicit, finite-difference method that is forward in time and centered in space (Eqs. (6) – (8)). Each pipeline of length L is discretized into a number of elements equal to $J = \lceil L/\Delta x \rceil$, resulting in a uniform mesh of $J+1$ nodes. Variables are stored at the boundary of the i-th volume element $(x, x+1)$ and evaluated at its midpoint. For each pipeline, the following equations can be written, where t and x denote time and space discretization.

$$\frac{(\rho_{\mathrm{x+1}}^{\mathrm{t}} - \rho_{\mathrm{x+1}}^{\mathrm{t-1}} + \rho_{\mathrm{x}}^{\mathrm{t}} - \rho_{\mathrm{x}}^{\mathrm{t-1}})}{2\Delta t} + \frac{(\dot{m}_{\mathrm{x+1}}^{\mathrm{t}} - \dot{m}_{\mathrm{x}}^{\mathrm{t}})}{\Delta x \mathrm{A}} = 0\,, \tag{6}$$

$$\frac{(p_{\mathrm{x+1}}^{\mathrm{t}} - p_{\mathrm{x}}^{\mathrm{t}})}{2\Delta x} + \frac{(\dot{m}_{\mathrm{x+1}}^{\mathrm{t}} - \dot{m}_{\mathrm{x+1}}^{\mathrm{t-1}} + \dot{m}_{\mathrm{x}}^{\mathrm{t}} - \dot{m}_{\mathrm{x}}^{\mathrm{t-1}})}{4A\Delta t} + \frac{2f(\dot{m}_{\mathrm{x}}^{\mathrm{t}} + \dot{m}_{\mathrm{x+1}}^{\mathrm{t}})^2}{\pi^2 D^5(\rho_{\mathrm{x+1}}^{\mathrm{t}} + \rho_{\mathrm{x}}^{\mathrm{t}})} = 0\,, \tag{7}$$

$$\frac{(\rho_{\mathrm{x}}^{\mathrm{t}} + \rho_{\mathrm{x+1}}^{\mathrm{t}})\left(c_{\mathrm{m,x+1}}^{\mathrm{t}} - c_{\mathrm{m,x+1}}^{\mathrm{t-1}} + c_{\mathrm{m,x}}^{\mathrm{t}} - c_{\mathrm{m,x}}^{\mathrm{t-1}}\right)}{4\Delta t} + \frac{(\dot{m}_{\mathrm{x}}^{\mathrm{t}} + \dot{m}_{\mathrm{x+1}}^{\mathrm{t}})\left(c_{\mathrm{m,x+1}}^{\mathrm{t}} - c_{\mathrm{m,x}}^{\mathrm{t}}\right)}{2A\Delta x} = 0\,. \tag{8}$$

Nodes are elements of gas networks acting as connection points between various pipelines. At each node, a mass balance equation is applied (Eq. (9)), which states that, given a time-step t, the sum of all inflow and outflow mass rates of the node equals zero. For each time-step t, the balance is mathematically described by the following equation

https://doi.org/10.52202/077185-0007

$$\sum_{\mathrm{i}} \dot{m}_{\mathrm{i}}^{\mathrm{t}} - \sum_{\mathrm{j}} \dot{m}_{\mathrm{j}}^{\mathrm{t}} + \dot{m}_{\mathrm{H_2,inj}}^{\mathrm{t}} + \dot{m}_{\mathrm{s}}^{\mathrm{t}} = \dot{m}_{\mathrm{dmd}}^{\mathrm{t}} \,, \tag{9}$$

where $\dot{m}_{\mathrm{i}}^{\mathrm{t}}$ and $\dot{m}_{\mathrm{j}}^{\mathrm{t}}$ represent all the incoming and outgoing pipe mass flow rates in the node, respectively, while $\dot{m}_{\mathrm{dmd}}^{\mathrm{t}}$ is the required gas mixture demand, $\dot{m}_{\mathrm{s}}^{\mathrm{t}}$ the natural gas supplied to the node and $\dot{m}_{\mathrm{H_2,inj}}^{\mathrm{t}}$ the hydrogen mass flow rate injected into the node. In addition, considering the presence of localized hydrogen injection, the mass balance must also be written for the hydrogen gas component, as follows

$$\sum_{\mathrm{i}} c_{\mathrm{m,i}} \dot{m}_{\mathrm{i}}^{\mathrm{t}} - c_{\mathrm{m,j}} \sum_{\mathrm{j}} \dot{m}_{\mathrm{j}}^{\mathrm{t}} + \dot{m}_{\mathrm{H_2,inj}}^{\mathrm{t}} = c_{\mathrm{m,j}} \dot{m}_{\mathrm{dmd}}^{\mathrm{t}} \,, \tag{10}$$

with c_{m} being the hydrogen mass fraction. According to an energy-based approach, to ensure energy demand fulfillment at each time-step, when a mixture of NG-H_2 replaces only NG, the relationship between mass demand $\dot{m}_{\mathrm{dmd}}^{\mathrm{t}}$ and original demand $\dot{m}_{\mathrm{NG,dmd}}^{\mathrm{t}}$ is defined as follows

$$\dot{m}_{\mathrm{dmd}}^{\mathrm{t}} = \frac{\dot{m}_{\mathrm{NG,dmd}}^{\mathrm{t}} \, HHV_{\mathrm{NG}}}{c_{\mathrm{m,j}} \, HHV_{\mathrm{H_2}} + \left(1 - c_{\mathrm{m,j}}\right) HHV_{\mathrm{NG}}} \,. \tag{11}$$

By consolidating all equations into a closed algebraic formulation, the discretized system was solved using a simultaneous solution approach.

2.1.2 Energy system components

As mentioned above, the novel control strategy is applied in an MiL configuration to a detailed model of the system. Besides the model of the gas distribution network, a detailed mathematical model is also developed for the other components of the system, namely an electrolyzer and a wind farm. The models are implemented in the MATLAB®/Simulink® environment, and they are part of a library of energy system components developed in-house (Marzi *et al.*, 2023). The models employed in this work are summarized in the following paragraphs.

Wind farm: this model is developed as an algebraic model. It calculates the electrical power output of the wind farm starting from the geometry of the wind turbines, their position in the wind farm and the undisturbed wind velocity module and direction. It takes into consideration the wake effect that the wind turbines exert on the nearby turbines by applying the Jensen wake model (Yang *et al.,* 2019).

PEM electrolyzer: this model is developed as an algebraic model. It calculates the amount of hydrogen and the thermal power generated by the electrolyzer, with a given electrical power input. It models three different operating modes: on, off (i.e. no production, no consumption, cold start-up to switch on) and standby (i.e. no production, consumption of small amount of electricity, warm start-up to switch on). To model the steady-state operation, the relationships were derived by interpolating operating data from the literature (see Marzi *et al.*, 2023).

2.2 Model Predictive Control

The MPC strategy is a smart control strategy which has already been demonstrated to be successful in many applications. When using this type of controllers, at every time-step the controller receives the states of the system and the information regarding the future disturbances influencing its behavior as inputs. By using optimization algorithms with an integrated simplified model of the system to control, the controller enables the prediction and calculation of the optimal trajectory of inputs over the prediction horizon. Among these inputs, only those corresponding to the first time-step are actually applied to the system. After one time-step has passed, the prediction horizon is moved forward by one time-step and the calculation is repeated for the new prediction horizon.

This method enables the optimal control of complex systems and, by updating the parameters at every time-step, it allows optimal real-time management. In addition, the uncertain behavior of the disturbances can be tackled by updating them at every time-step based on real-time forecasts, or by using a stochastic optimization approach in the controller. However, the algorithms used need to be fast, in order for the controller to work in real-time. For this application, two optimization algorithms are employed to cope with this task. Notably, the problem was divided into two sub-problems, one is dedicated to the natural gas network, and the other aims at optimizing the Multi-Energy System (MES)

https://doi.org/10.52202/077185-0007

in which hydrogen is generated. First, a Nonlinear Programming (NLP) algorithm, which optimizes the natural gas network, calculates the maximum amount of hydrogen that can be injected into the network during the prediction horizon, in order to meet the maximum concentration constraint. Afterwards, this information is read by a Mixed-Integer Linear Programming (MILP) algorithm, which transforms it into an upper bound for the electrolyzer operation and calculates the optimal management for the whole system. The strong coupling and the dynamic characteristics of integrated energy systems with blending of hydrogen make it challenging to set an optimal control for the system, which is able to optimally manage the system in real-time. To make it possible, the model used in the optimization algorithms embedded in the MPC are simplified. In this way, the computational time needed to find the optimal solution is suitable for a real-time control of the system.

For developing the NLP algorithm, the equations describing gas motion (Eqs. (1) and (2)) were further simplified, according to common operating conditions. Particularly, the time derivative term in Eq. (2) was omitted, having a negligible effect on the solution under common flow conditions (Correa-Posada *et al.*, 2014). Assuming a unidirectional flow, the resulting equations are the following

$$\dot{m}^{\mathrm{t}}_{\mathrm{x+1}} - \dot{m}^{\mathrm{t}}_{\mathrm{x}} = \frac{\pi}{4}\frac{\Delta x D^2}{R_{\mathrm{g}} T Z \Delta t}\left(p^{\mathrm{t-1}}_{\mathrm{x,x+1}} - p^{\mathrm{t}}_{\mathrm{x,x+1}}\right), \tag{12}$$

$$\left(\dot{m}^{\mathrm{t}}_{\mathrm{x,x+1}}\right)^2 = \left(\frac{\pi}{4}\right)^2 \frac{D^5}{\Delta x f R_{\mathrm{g}} T Z}\left[(p^{\mathrm{t}}_{\mathrm{x}})^2 - (p^{\mathrm{t}}_{\mathrm{x+1}})^2\right], \tag{13}$$

where $\dot{m}^{\mathrm{t}}_{\mathrm{x,x+1}}$ and $p^{\mathrm{t}}_{\mathrm{x,x+1}}$ represent the average mass flow rate and pressure in the pipe segment $(x, x+1)$, respectively. Eqs. (9) – (11) are used for node balances and to model end-user demand fulfilment.

To track the hydrogen concentration in the pipeline, the batch tracking method was employed (Chaczykowski *et al.*, 2018). A schematic representation of this method is shown in Figure 1.

At the initial time-step, the system is initialized with a large batch filling the entire pipe. Then, at each time-step, a new batch enters the injection point. It is assumed that a single batch b_{k} of constant H_2 mass fraction equal to $c_{\mathrm{m,b_k}} = m^{\mathrm{t_0}}_{\mathrm{H_2}}/(m^{\mathrm{t_0}}_{\mathrm{H_2}} + m^{\mathrm{t_0}}_{\mathrm{NG}})$ enters the injection point at every time-step, and its position $\delta_{\mathrm{b_k}}$ in the pipe is tracked over time. The initial position of the batch is calculated as

$$\delta^{\mathrm{t_0}}_{\mathrm{b}_k} = \frac{m^{\mathrm{t_0}}_{\mathrm{H_2}}}{\rho^{\mathrm{t_0}}_{\mathrm{H_2}} A} + \frac{m^{\mathrm{t_0}}_{\mathrm{CH_4}}}{\rho^{\mathrm{t_0}}_{\mathrm{NG}} A}, \tag{14}$$

where t_0 represents the time-step in which the batch enters the pipe and $m^{\mathrm{t_0}}_{\mathrm{z}}$ the total mass of component z entered during the time-step length. Then, the batch position is tracked by using the following equation

$$\delta^{\mathrm{t}}_{\mathrm{b_k}} = \delta^{\mathrm{t}}_{\mathrm{b_{k+1}}} + \delta^{\mathrm{t_0}}_{\mathrm{b_k}} \frac{p^{\mathrm{t_0}}}{p^{\mathrm{t}}_{\mathrm{x,x+1}}}, \tag{15}$$

where $\delta^{\mathrm{t}}_{\mathrm{b_{k+1}}}$ denotes the position of the batch injected during the time-step after batch b_{k}, $p^{\mathrm{t_0}}$ is the initial batch pressure while $p^{\mathrm{t}}_{\mathrm{x,x+1}}$ is the average pressure of the grid cell in which $\delta^{\mathrm{t}}_{\mathrm{b_k}}$ is located. The algorithm decision variables are the mass flow rates and pressures of the network, and it aims at minimizing or maximizing the implemented cost function.

The second algorithm embedded in the controller is an MILP algorithm. It was already tested and validated as an optimization tool in an MPC for different applications in Marzi *et al.* (2023) and Marzi *et al.* (2024), and it proved to be effective in optimizing MES management, if properly tailored to the case study. It computes the optimal energy flows in the system over the prediction horizon considered, minimizing a certain objective function. The algorithm tackles the dynamics of the system by modeling energy exchanges with end-users and external networks, renewable generation, when available, and

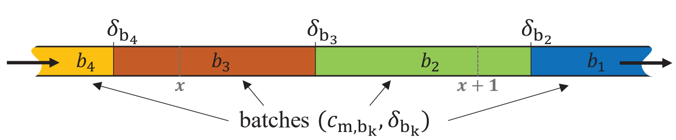

Figure 1: Schematic representation of batch positions $\delta_{\mathrm{b_k}}$ and composition $c_{\mathrm{m,b_k}}$ (the different colors represent the different gas composition in each batch); x and $x+1$ are the grid points.

https://doi.org/10.52202/077185-0007

conversion unit operation, using piecewise linearization for modeling variations in efficiency with the load and different operating modes for each of them.

3 APPLICATION

This section presents the case study analyzed in this work, how the MPC strategy was applied to it and its implementation in the MiL configuration.

3.1 Case study description

The case study is schematically represented in Figure 2. It comprises a 25-km natural gas distribution network with three nodes: node 1 (N1) is an NG supply node (5 bar), node 2 (N2) allows the injection of hydrogen, while node 3 (N3) represents the user node, with a fuel demand profile associated to it. The diameter of the pipeline is set equal to $D = 0.3$ m, while the relative roughness is assumed equal to $\varepsilon/D = 0.005$. The ambient temperature is considered constant and equal to 15 °C.

The case study also comprises a wind farm, with peak power of 8000 kW, for renewable electricity generation, and a PEM electrolyzer, with nominal power equal to 3750 kW, which allows the conversion of the renewable energy into hydrogen, for injection into the natural gas network in N2. In addition, the system is connected to the electrical grid, with which it can exchange electricity by buying or selling it, and it has an electrical end-user. It is assumed that the natural gas entering N1 corresponds to the *Nord European* gas, as identified by Guzzo *et al.* (2022). Therefore, to fulfil the gas quality parameter limits imposed by the Italian regulation, which constrains the Wobbe Index, specific gravity and Higher Heating Value of the gas, a maximum molar concentration of hydrogen in the gas equal to 9.7 % is allowed. This corresponds to a maximum allowable mass fraction of 1.23 %, according to

$$c_{\mathrm{v}} = \left(1 - \frac{\rho_{\mathrm{std,H_2}}}{\rho_{\mathrm{std,NG}}} + \frac{\rho_{\mathrm{std,H_2}}}{\rho_{\mathrm{std,NG}}} c_{\mathrm{m}}^{-1}\right)^{-1}. \tag{16}$$

3.2 Implementation

The MPC was implemented in an MiL configuration. At every time-step, the controller (i) receives information regarding the state of the system from the model; (ii) performs the optimization procedure; and (iii) returns the optimal inputs for the next time-step to the system. This procedure is schematically represented in Figure 3. The controller takes as inputs the node pressures, the electrolyzer state, and the amount of hydrogen and natural gas that entered N2 during the past time-step. In this way, it can compute the actual average concentration of the batch that entered pipe 2 during the previous time-step. This information is used as the initial state for the optimization. When the controller is called, the following steps are executed: (i) the NLP algorithm is run and computes the maximum amount of hydrogen that can be injected over the prediction horizon; (ii) it communicates this information to the MILP algorithm, which uses it as an upper bound for the electrolyzer operation over the prediction horizon; (iii) the MILP optimization is performed; and (iv) the set-point for the electrolyzer is communicated to the system model, which uses it for the next time-step.

As mentioned above, the NLP model aims at maximizing the amount of hydrogen injected into the network, and therefore at keeping the concentration of the mixture at the user node at the maximum value allowed, i.e. $c_{\mathrm{v}} = 9.7$ %.

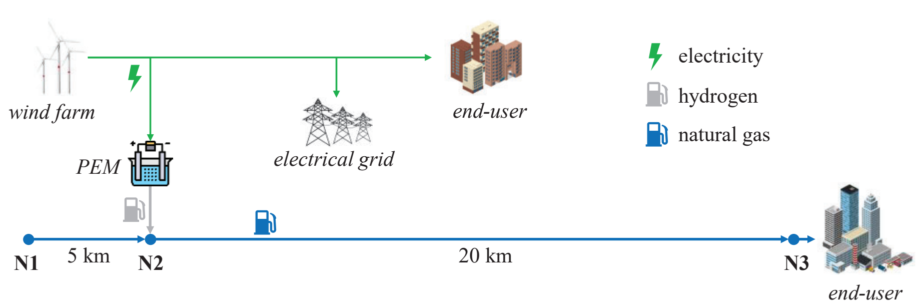

Figure 2: Schematic representation of the case study considered.

https://doi.org/10.52202/077185-0007

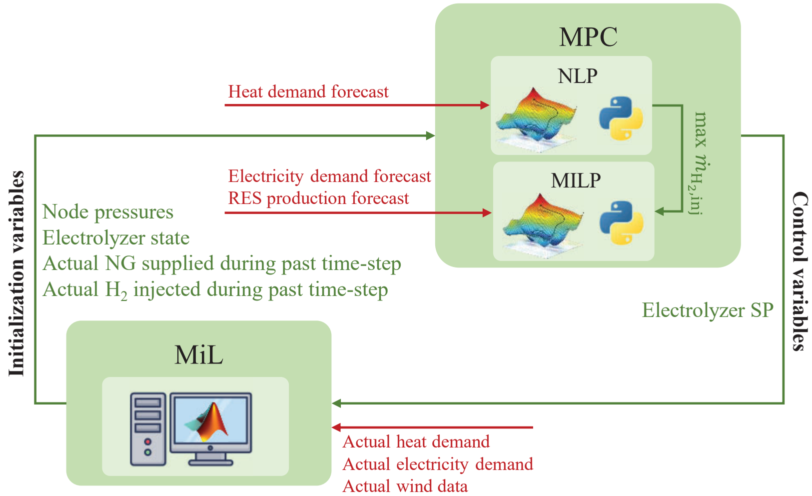

Figure 3: Diagram of Model-in-the-Loop implementation of the controller (SP = set-point).

To this end, at every time-step the controller computes the concentration of the gas entered during the past time-step, by using actual data from the system, and it uses this information for decision-making. As the controller uses a simplified model of the system and a forecast of disturbances that may be different from those that actually occur, the concentration of the previous batch may be higher than the set limit. In such circumstances, the controller compensates this error by lowering the maximum concentration of the next batch. In particular, it sets as a constraint in the NLP optimization

$$c_{\mathrm{m,b_k}} \leq 2c_{\mathrm{m,b,lim}} - \tilde{c}_{\mathrm{m,b_{k+1}}} \,, \tag{17}$$

where $c_{\mathrm{m,b,lim}}$ represents the concentration limit, $c_{\mathrm{m,b_k}}$ is the concentration of the batch entering the pipe at the next time-step and $\tilde{c}_{\mathrm{m,b_{k+1}}}$ is the measured concentration of the batch that entered the pipe during the past time-step. This imposes the average concentration of the two batches to be equal to the limit $c_{\mathrm{m,b,lim}}$, and therefore to lower the concentration of the next batch in order to compensate for the inaccuracy occurred in the previous time-step. Indeed, even though no mixing among batches is assumed with the batch approach, the compensation works in real gas mixtures, when gas mixing actually occurs to some extent.

The simulations were carried out over a period of one day. The controller is set with a prediction horizon of 12 hours and a time-step of 30 minutes. The disturbances given to it are the forecasts of the end-users' electrical and thermal needs and of the renewable energy generation. They are represented in Figure 4 for the simulated day. It was assumed that the renewable energy generated by the wind farm is associated with an electrical end-user and that the surplus renewable energy can be injected into a distribution natural gas network, which supplies the gas to a larger neighborhood. It is worth mentioning that the forecasts given to the MPC controller are different from the disturbances applied to the Simulink® model. Indeed, the latter depict the actual disturbances, and they are generated by introducing random deviations to the ideal disturbances provided to the controller. This approach enables the assessment of the response of the predictive controller to unexpected disturbances, mirroring real-world scenarios. The gas network model presented in Paragraph 2.1.1 was set with a time discretization of 300 s and a space discretization of 1000 m. In order to reduce the number of variables, the MPC instead works with a time-step of 30 minutes and the space discretization for the gas network is set to 5000 m. Indeed, from preliminary simulations it was found that longer time-steps do not allow a proper real-time control of the system.

As the controller operates with two optimization algorithms, two objectives are implemented. The objective of the NLP algorithm is the maximization of the amount of hydrogen injected over the prediction horizon, and it is represented by the following equation

$$\max f_{\mathrm{obj_{NLP}}} = \max \textstyle\sum_{t=1}^{N_{\mathrm{t}}} \dot{m}_{\mathrm{H_2,inj}}^{\mathrm{t}} \,, \tag{18}$$

https://doi.org/10.52202/077185-0007

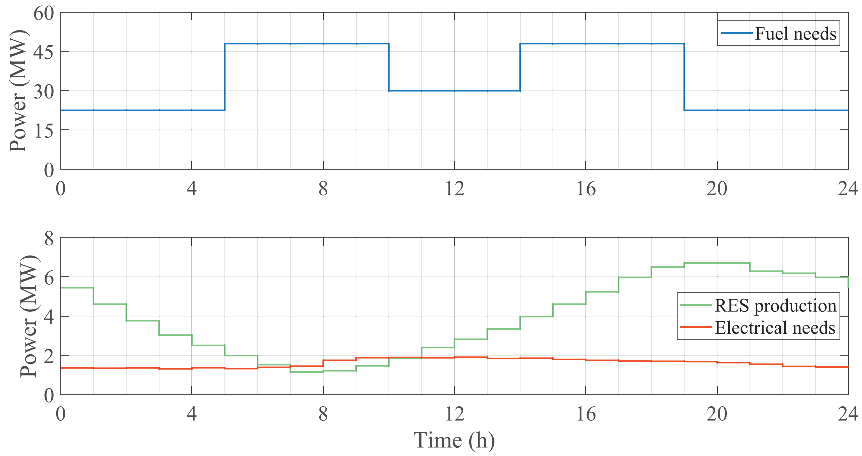

Figure 4: Forecast of disturbances given to the MPC controller.

where $\dot{m}^{\mathrm{t}}_{\mathrm{H_2,inj}}$ is the average hydrogen mass flow rate injected into N2 during time-step t and N_{t} is the total number of time-steps of the prediction horizon.

The objective function of the MILP algorithm instead consists of the minimization of electricity exchanges with the electricity grid, i.e. the maximization of electricity used by the system. Indeed, when considering the integration of distributed RES within the grid, the injection of high amount of electricity can cause grid instability issues. The objective function is expressed by the following equation

$$\min f_{\mathrm{obj_{MILP}}} = \min \sum_{t=1}^{N_{\mathrm{t}}} [P^{\mathrm{t}}_{\mathrm{el,bo}} + P^{\mathrm{t}}_{\mathrm{el,so}}]\, \Delta t \,, \tag{19}$$

where $P^{\mathrm{t}}_{\mathrm{el,bo}}$ and $P^{\mathrm{t}}_{\mathrm{el,so}}$ are the average amount of electricity bought and sold to the network during time-step t, respectively, and Δt is the time-step length.

4 RESULTS AND DISCUSSION

To test the novel control on the model of the system using the architecture presented in the previous section, two simulations have been carried out. In the first simulation, the system is tested considering an unlimited availability of renewable energy (Renewable Energy Unconstrained – REU simulation), while for the second simulation, the disturbances shown in Figure 4 are used for wind energy generation (Renewable Energy Constrained – REC simulation).

Figure 5 displays the pressure at the nodes and the total mass flow rate exiting the three nodes during the simulated day in the REU simulation. In Figure 6, the hydrogen injected over the simulated day and the resulting hydrogen concentration at node N3 is depicted. It can be seen that, as expected, at every time-step the maximum allowed amount of hydrogen is injected, and the concentration is maintained as close as possible to the set limit. Thanks to the use of the novel controller, it is possible to manage the electrolyzer in such a way that the concentration is maintained under the set limit. Indeed, as discussed in Paragraph 3.2, the controller is able to adjust its operation based on feedback from the system and vary the injection of hydrogen according to that.

The results of the REC simulation are showed in Figure 7 and 8. Figure 7 shows how the electricity is managed within the system during the simulated day: it displays the energy balance among production, usage and energy exchange with the grid. It can be noted that, as the objective of the controller is to minimize energy exchanges with the electricity grid, when the renewable energy is not in surplus, the electrolyzer is switched off and the renewable energy is used to fulfill the electrical needs.

As a result, as depicted in Figure 8, when the electrolyzer is switched off, the hydrogen concentration in the pipes drops to zero. Nevertheless, the controller is able to handle variations in hydrogen concentration, and restore the concentration as soon as the renewable energy is available.

When looking at cumulative results over the simulated day, it is obtained that in the REU simulation, without a limit on renewable energy production, the CO_2 emissions associated with end-user fuel

https://doi.org/10.52202/077185-0007

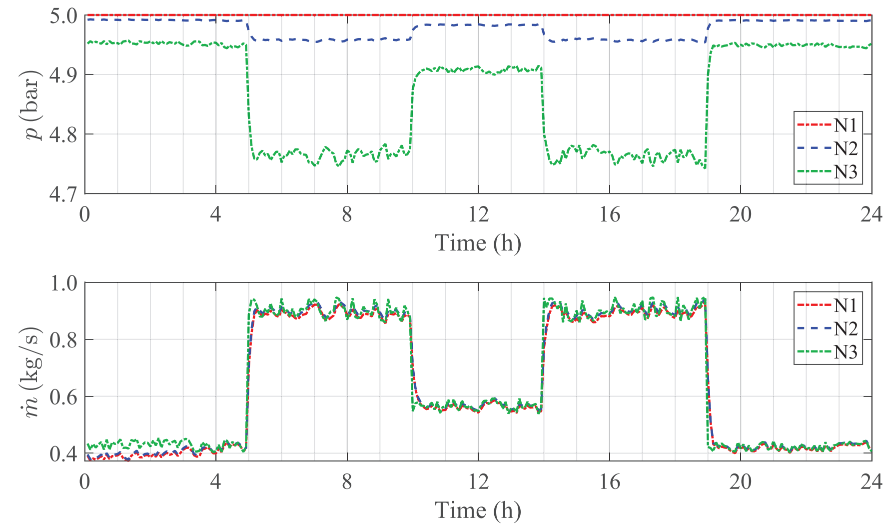

Figure 5: Pressure at the nodes and total mass flow rate exiting the nodes during the simulated day in the REU simulation.

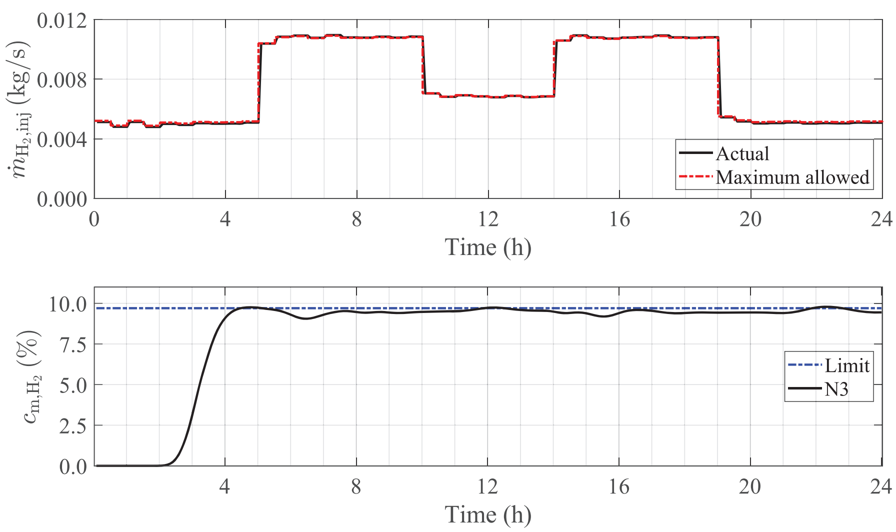

Figure 6: Hydrogen injected and hydrogen molar concentration during the simulated day in the REU simulation.

demand are reduced by 2.9 %, if compared to the case in which the fuel needs are fulfilled only by using natural gas. This number drops to 1.8 % of the reduction in CO_2 emissions in the REC simulation, as the electrolyzer is switched off during part of the day, due to limited renewable energy availability.
The case study analyzed presents a straightforward scenario, ideal for initial testing of the developed MPC control strategy. In such system, employing a PID controller to regulate hydrogen injection might also be feasible, with the aim of keeping hydrogen concentration constant by monitoring hydrogen and natural gas flows. Nonetheless, when more complex networks are analyzed, e.g. with multiple injection or mixing points and diverse end-users, the ability of the controller to have a holistic view of the system is of crucial importance to ensure compliance with concentration and pressure limits in the network. In such configurations, the novel MPC could be integrated with lower-level conventional controllers and communicate the operational set-points to them.

https://doi.org/10.52202/077185-0007

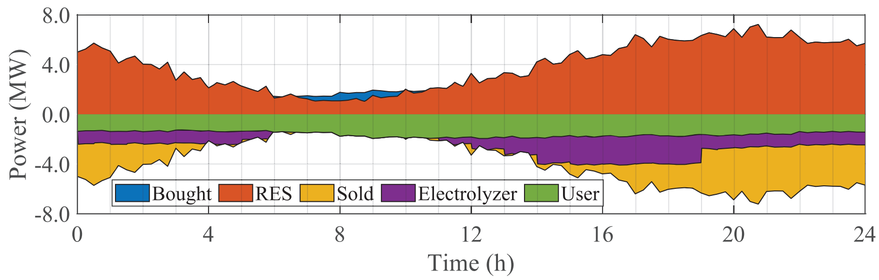

Figure 7: Electricity balance in the system during the simulated day in the REC simulation.

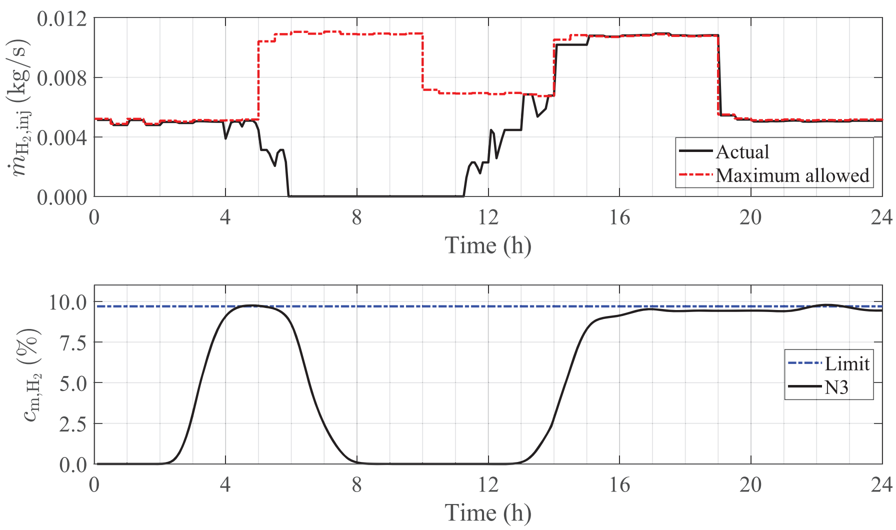

Figure 8: Hydrogen injected and hydrogen molar concentration during the simulated day in the REC simulation.

5 CONCLUSIONS

Many efforts are being made to foster the integration in the current energy systems of novel technologies to enable the decarbonization of various sectors. In this context, Power-to-Gas solutions allow sector integration and the production of green fuels such as green hydrogen from surplus renewable electricity. Nonetheless, the use of existing infrastructures is crucial to accelerate the transition toward a fully decarbonized system. In this framework, hydrogen injection into the existing natural gas network can foster the production and use of green hydrogen for decarbonizing many hard-to-electrify sectors. Nevertheless, for the safe operation of the network and user appliances, limits on hydrogen concentration in the gas mixture need to be set. To optimally manage the production and injection of hydrogen into the network, a control for the system is needed, which can tackle the dynamics of the entire energy system and ensure compliance with regulatory limits on hydrogen concentration.
In this work, an innovative control strategy based on Model Predictive Control is developed for optimally managing the generation of green hydrogen through an electrolyzer and its direct injection into the natural gas network. Notably, the controller was tested in a Model-in-the-Loop configuration for the optimal management of an electrolyzer and the direct injection of hydrogen into the gas network. The controller is able to manage the electrolyzer in real-time, relying on a simplified model of the system to control and using data on the actual behavior of the system at every time-step to adjust its operation. The results show that the developed control strategy enables the optimal injection of hydrogen, keeping the gas concentration under the set limit, and to maximize the usage of renewable energy, when available, reducing carbon dioxide emissions. Future studies will investigate various systems, which can include many end-users, multiple hydrogen injection points and hydrogen storage units, to analyze whether the controller can be adapted to more complex systems.

https://doi.org/10.52202/077185-0007

NOMENCLATURE

A	Pipe area	(m^2)
c_{m}	H_2 mass fraction	(–)
c_{v}	H_2 molar fraction	(–)
D	Pipe diameter	(m)
f_{obj}	Objective function	
f	Friction factor	(–)
g	Gravitational acceleration	(m/s^2)
HHV	Higher Heating Value	(MJ/kg)
J	Set of pipe segments	
L	Pipe length	(m)
m	Mass	(kg)
$\dot{m}$	Mass flow rate	(kg/s)
MES	Multi-Energy Systems	
MiL	Model-in-the-Loop	
MILP	Mixed-Integer Linear Programming	
MPC	Model Predictive Control	
NLP	Nonlinear Programming	
NG	Natural Gas	
N_{t}	Number of time-steps	
P	Power	(MW)
p	Pressure	(Pa)
PEM	Proton Exchange Membrane	
R_{g}	Gas constant	(J /(kg K))
REC	Renewable Energy Constrained	
RES	Renewable Energy Source	
REU	Renewable Energy Unconstrained	
SP	Set-point	
T	Temperature	(K)
Z	Compressibility factor	(–)
ε	Pipe roughness	(m)
ρ	Density	(kg/m^3)
δ	Batch position in the pipeline	(m)
θ	Pipe inclination angle	(deg)
Δt	Time discretization length	(s)
Δx	Space discretization length	(m)

Subscripts and superscripts

b	batch
bo	bought
dmd	demand
el	electricity
g	gas
i	i-th pipe incoming flow in a node
inj	injected
j	j-th pipe outgoing flow in a node
k	index for batch
lim	limit
s	supplied
so	sold
std	standard
t	index for time discretization
x	index for spatial discretization

https://doi.org/10.52202/077185-0007

REFERENCES

Cadorin, M., Morini, M., Pinelli, M., 2010, Numerical analyses of high Reynolds number flow of high pressure fuel gas through rough pipes, *Int. J. Hydrogen Energ.*, vol. 35, no. 14: p. 7568-7579.

Chaczykowski, M., Sund, F., Zarodkiewicz, P., Hope, S. M., 2018, Gas composition tracking in transient pipeline flow, *J. Nat. Gas Sci. Eng*, vol. 55: p. 321-330.

Cheli, L., Guzzo, G., Adolfo, D., Carcasci, C., 2021, Steady-state analysis of a natural gas distribution network with hydrogen injection to absorb excess renewable electricity, *Int. J. Hydrogen Energ.*, vol. 46, no. 50: p. 25562-25577.

Correa-Posada, C. M., & Sánchez-Martín, P., 2014, Gas network optimization: A comparison of piecewise linear models, *Optimization Online*: p. 1-24.

Cristello, J. B., Yang, J. M., Hugo, R., Lee, Y., Park, S. S., 2023, Feasibility analysis of blending hydrogen into natural gas networks, *Int. J. Hydrogen Energ.*, vol. 48 no. 46: p. 17605-17629.

Erdener, B. C., Sergi, B., Guerra, O. J., Chueca, A. L., Pambour, K., Brancucci, C., Hodge, B. M., 2023, A review of technical and regulatory limits for hydrogen blending in natural gas pipelines. *Int. J. Hydrogen Energ.*, vol. 48, no. 14: p. 5595-5617.

Guandalini, G., Colbertaldo, P., Campanari, S., 2017, Dynamic modeling of natural gas quality within transport pipelines in presence of hydrogen injections, *Appl. Energy*, vol. 185: p. 1712-1723.

Guzzo, G., Cheli, L., Carcasci, C., 2022, Hydrogen blending in the Italian scenario: Effects on a real distribution network considering natural gas origin. *J. Clean. Prod.*, vol. 379: 134682.

Isaac, T., 2019, HyDeploy: The UK's first hydrogen blending deployment project, *Clean Energy*, vol. 3 no. 2: p. 114-125.

Marzi, E., Gambarotta, A., Ghionda, F., Morini, M., Saletti, C., 2023, Optimal integration of Power-to-Gas and district heating through waste heat recovery from electrofuel production. *Proceedings of ECOS 2023 – The 36th International Conference on Efficiency, Cost, Optimization, Simulation and Environmental Impact of Energy Systems*: p. 2456-2467.

Marzi, E., Morini, M., Saletti, C., & Gambarotta, A., 2024, Coordinating multiple Power-To-Gas plants for optimal management of e-fuel seasonal storage. *Smart Energy*, 100143.

Menon, E. S., 2005, *Gas pipeline hydraulics*, Boca Raton FL, US: CRC Press, Taylor & Francis Group.

Mhanna, S., Saedi, I., Mancarella, P., & Zhang, Z., 2022, Coordinated operation of electricity and gas-hydrogen systems with transient gas flow and hydrogen concentration tracking, *Electr. Power Syst. Res.*, vol. 211: 108499.

Morini, M., Pinelli, M., Venturini, M., 2009, Analysis of biogas compression system dynamics, *Appl. Energy*, vol. 86, no. 11: p. 2466-2475.

Neumann, F., Zeyen, E., Victoria, M., Brown, T., 2023, The potential role of a hydrogen network in Europe, *Joule*, vol. 7, no. 8: p. 1793-1817.

Soave, G., 1972, Equilibrium constants from a modified Redlich-Kwong equation of state, *Chem. Eng. Sci.*, vol. 27, no. 6: p. 1197-1203.

Yang, K., Kwak, G., Cho, K., Huh, J., 2019, Wind farm layout optimization for wake effect uniformity, *Energy*, vol. 183: p. 983-995.

Zhang, Z., Saedi, I., Mhanna, S., Wu, K., Mancarella, P., 2022, Modelling of gas network transient flows with multiple hydrogen injections and gas composition tracking, *Int. J. Hydrogen Energ.*, vol. 47, no. 4: p. 2220-2233.

Zhou, D., Jia, X., Peng, Z., Ma, Y., 2022, Coordinate control law analysis for hydrogen blended electricity-gas integrated energy system, *Int. J. Hydrogen Energ.*, vol. 47 no. 69: p. 29648-29660.

ACKNOWLEDGEMENTS

This work was supported by the National Recovery and Resilience Plan (NRRP) with the project "Ecosystem for Sustainable Transition in Emilia-Romagna" (Ecosister), Mission 4 Component 2 Investment 1.5 (project code ECS00000033) and the project "Network 4 Energy Sustainable Transition – NEST", Mission 4 Component 2 Investment 1.3, (project code PE0000021). Projects funded by the European Union – NextGenerationEU. This work was co-authored by a researcher with a research contract co-funded by the European Union – PON Ricerca e Innovazione 2014-2020.

https://doi.org/10.52202/077185-0007